SEMARAK ILMU PUBLISHING

Journal of Advanced Research in Fluid Mechanics and Thermal Sciences

Journal homepage:
https://semarakilmu.com.my/journals/index.php/fluid_mechanics_thermal_sciences/index
ISSN: 2289-7879

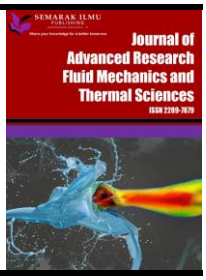

Thin-Layer Drying of Burdock Root in a Convective Dryer: Drying Kinetics and Numerical Simulation

Luan Thanh Nguyen[1,*], Minh Ha Nguyen[2], Hong Son Nguyen Le[1]

[1] Faculty of Vehicle and Energy Engineering, Ho Chi Minh City University of Technology and Education (HCMUTE), Vietnam
[2] Faculty of Mechanical Engineering, University of Transport and Communications, Hanoi, Vietnam

ARTICLE INFO

Article history:
Received 30 October 2022
Received in revised form 7 February 2023
Accepted 15 February 2023
Available online 5 March 2023

Keywords:
Burdock root (Arctium lappa); thin-layer drying; convective dryer; drying kinetics; moisture diffusivity coefficient; moisture transfer coefficient; numerical simulation

ABSTRACT

This work investigated the thin-layer drying kinetics of Vietnam burdock root in a convective dryer. The thin-layer drying models and mass transfer coefficient were determined by experiment and analysis approach. Furthermore, a numerical simulation was performed to describe the moisture distribution inside the material. The regression models and mathematical equations were determined by Statgraphics software and the EES software. The survey range in this work: 50–70^{o}C air temperature, 1–2 m/s air velocity, 22 ± 5 mm slice diameter, and 5 ± 0.2 mm slice thickness. The results show that the Page model was the best model to describe the drying behavior of burdock root, with the correlation coefficient of $R^2 > 0.9992$; the moisture diffusivity coefficient $D_e = 3.4520 \times 10^{-9}$–$1.8516 \times 10^{-8}$ m^2/s; moisture transfer coefficient $h_m = 1.3256 \times 10^{-7}$–$7.8375 \times 10^{-7}$ m/s. Furthermore, the simulation results visualize the moisture distribution inside the burdock root slice in the drying process.

1. Introduction

Burdock is a herb that belongs to the Asteraceae family. It is used in traditional medicine and daily food in many countries in Asia, including Vietnam. Burdock root is cylindrical and contains many proteins, starches, microelements, and amino acids. It has detoxifying, anti-inflammatory, and antioxidant properties [1]. Therefore, the potential use of burdock root is explored and used in many applications. For instance: the production of burdock oil, burdock tea, and burdock wine or used in traditional medicine to treat colds, oedema, and anti-inflammatory.

Fresh Burdock root has a high moisture content. It is favorable for the growth of fungi and microorganisms. Drying is a technique to preserve the quality of the product. It is an important step in the production of Burdock products because it extends the shelf life. The drying properties of burdock roots have been examined in many studies. Lu *et al.,*[2] compared the color and flavor of dried burdock root in a convective dryer and the microwave-combined fluidized bed dryer. They reported that the dried sample in a convective dryer was better color and esters than those in a

* *Corresponding author.*
E-mail address: luannt@hcmute.edu.vn

https://doi.org/10.37934/arfmts.104.1.2136

microwave-combined fluidized bed dryer. Xia *et al.,*[3] investigated the effect of drying methods on the volatile component of burdock root. They reported that the dried product in a convective dryer and vacuum dryer had the highest volatile components. Zang *et al.,*[4] evaluated the color and quality of dried burdock root in a convective dryer. They reported that the highest color fastness and chlorogenic acid content could be obtained at 60^{o}C and 70^{o}C–80^{o}C, respectively. The above studies showed that the drying characteristics of burdock root had been investigated in many aspects.

Drying is a complex heat and mass transfer process. Therefore, the drying characteristics of each material in each type of dryer are often investigated experimentally. Mathematical models describing the drying process are analyzed based on experimental data. However, these models can only describe the average of drying characteristics of the material during the drying process. It is impossible to consider the moisture distribution inside the material in terms of space and time. In recent decades with the development of numerical simulation, many simulation studies have been carried out, which helps to reduce the time and cost of experiments. In particular, it can investigate the characteristics of heat transfer and mass transfer according to space and time that experiments can hardly be tested [5-7]. The application of numerical simulation to describe the moisture distribution inside materials during the drying process has been conducted in a few studies [8,9]. These studies performed based on boundary conditions are mass transfer parameters from the experimental data. The simulation results help to understand more deeply about mass transfer and moisture distribution inside materials at each time point.

This work aims to investigate the thin-layer drying kinetics of Vietnam burdock root in a convective dryer by considering the influence of 1–2 m/s air velocity and 50–70^{o}C drying temperature, which has not been found in previous studies. The first part of the paper focuses on determining the thin-layer drying model, moisture transfer coefficient, and moisture diffusivity coefficient according to the Bi-Di correlation. This correlation is used in many studies on the mass transfer process in drying techniques [10-12]. The second half of the paper presents the applying numerical simulation and mass transfer data to describe the moisture distribution inside the burdock root according to space and time in the drying process. The research results provide useful data for designing and operating a convective dryer to dry burdock roots.

2. Materials and Methods

2.1 Material

Fresh burdock roots (Figure 1) were selected with an average diameter of about 22 mm, then washed, drained, and sliced 5 ± 0.2 mm thickness. In the sample, slices were selected with 22 ± 5 mm diameter. The initial moisture content of the material was determined by the oven method [13, 14] at 105^{o}C for 24 hours, which was obtained as 0.77300 $\pm$ 0.00004 wet basis (w.b) or 3.4053 $\pm$ 0.0008 dry basis (d.b).

Fig. 1. Fresh burdock roots

2.2 Experiment Description

Figure 2 shows the convective dryer model. It is tailor-made with a mesh drying tray, and the airflow goes from the bottom up. The main technical parameters of the model are as follows: 200 x 200 x 300 mm drying chamber dimension, 85 W fan, and 4 kW resistor. Fan power and resistance are selected based on the test requirements. Fan speed is adjusted by dimmer; temperature and humidity are controlled and measured by FOX-300A-1 (temperature error ± 1%, humidity error ± 3%); air velocity is measured by PCE-007 (error ± 3%); the material is balanced by electronic balance (error ± 0.01 g); the material thickness is measured by electronic calipers (error ± 0.03 mm). The data were collected every 10 minutes, repeated thrice for each case, and the average for the data was taken. The test stops when the moisture content reaches below 0.12 w.b (0.136 d.b). This moisture avoids mold growth in tropical environmental conditions [15].

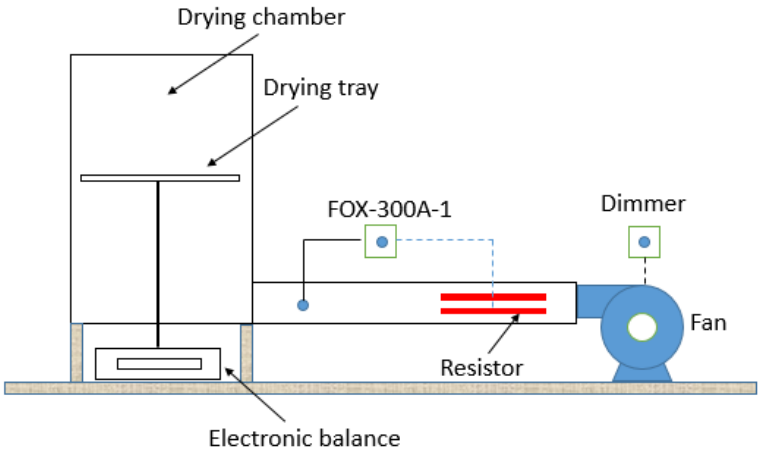

Fig. 2. Convective dryer model

2.3 Analytical Method

Moisture content wet basis can be determined [16]

$$W = \frac{g_{water}}{g_{material}} \tag{1}$$

where g_{water} (g) and $g_{material}$ *(g)* are the weight of water and materials at every time, respectively.

Moisture content dry basis is determined by the equation [17]

$$M = \frac{W}{1 - W} \tag{2}$$

The dimensionless moisture can be determined by the formula (ignoring equilibrium moisture) [8,11,18]

$$Y = \frac{M_i}{M_o} \tag{3}$$

In this work, the mass transfer coefficient is determined according to the Bi-Di correlation. This correlation is used in many studies related to the mass transfer process in the drying technique. In the range of the Biot number from 0.1 to 100, the calculation steps for mass transfer coefficient and reliability assessment are performed as follows [10].

Step 1: Determine the drying coefficient (s) and lag coefficient (C) in the equation Y = C.exp(-st), which is regression model from the experimental data.

Step 2: Calculate the characteristic roots parameter, for slab [10]

$$\zeta = -419.04C^4 + 2013.8C^3 - 3615.8C^2 + 2880.3C - 858.94 \quad (4)$$

Step 3: Calculate the Biot number and Dincer number [10]

$$Bi = 24.848Di^{-3/8} \quad (5)$$

$$Di = \frac{V}{s.L} \quad (6)$$

where L (m) and V(m/s) are the half-thickness of the material and air velocity.

Step 4: Calculate the moisture transfer coefficient (h_m) and moisture diffusivity coefficient (D_e) [10]

$$D_e = s.\frac{L^2}{\zeta^2} \quad (7)$$

$$h_m = \frac{D_e.Bi}{L} \quad (8)$$

Step 5: Calculate the dimensionless moisture according to the Bi-Di correlation and validation with the experimental data to evaluate the reliability of the mass transfer coefficient results [10]

$$Y = exp\left(\frac{0.2533Bi}{1.3 + Bi}\right).exp(st), \qquad for\ the\ slab \quad (9)$$

This study used five thin-layer drying models to choose the best model to describe the moisture reduction process, specifically as follows [17, 19]

i. Logarithmic model: $Y = m.exp(–st) + b$;
ii. Wang and Singh model: $Y = 1 + at + bt^2$;
iii. Lewis model: $Y = exp(-st)$;
iv. Henderson and Pabis model: $Y = m.exp(-st)$;
v. Page model: $Y = exp(-st^n)$.

The regression models were determined by Statgraphics software [20]. The fit of each model was evaluated based on three statistical criteria: the root means square error (RMSE), the reduced chi-square (χ^2), and the correlation coefficient (R^2). The RMSE represents the average deviations between predicted and experimental values. The χ^2 represents the mean square of the deviations between

predicted and experimental values, considering degrees of freedom. The R^2 represents the linear relation between experimental and predicted values [21]. The higher the R^2, the lower the RMSE, and the lower the χ^2, the better a model fits the experimental dataset.

The R^2, RMSE and χ^2 are determined by the formulas [4,21]

$$R^2 = 1 - \frac{\sum_{i=1}^{n}\left(Y_{pre}^{i} - Y_{exp}^{i}\right)^2}{\sum_{i=1}^{n}\left(Y_{exp}^{i} - Y_{exp}^{m}\right)^2} \tag{10}$$

$$RMSE = \sqrt{\frac{1}{n}\sum\nolimits_{i=1}^{n}\left(Y_{pre}^{i} - Y_{exp}^{i}\right)^2} \tag{11}$$

$$\chi^2 = \frac{1}{n-j}\sum\nolimits_{i=1}^{n}\left(Y_{pre}^{i} - Y_{exp}^{i}\right)^2 \tag{12}$$

where the n, Y_{pre}^{i}, Y_{exp}^{i}, Y_{exp}^{m} and j are the number of samples, the predicted value, the experimental value, the mean experimental value, and the number of variables in the regression model, respectively.

The uncertainty of the calculated results is determined [22]

$$U_R = \sqrt{\sum_{i}^{n}\left(\frac{\partial R}{\partial X_i}U_{X_i}\right)^2} \tag{13}$$

where R and U_{X_i} are the calculated result and the uncertainty in the measured quantity X_i. The uncertainty is calculated by the EES (Engineering Equation Solver) software [23].

3. Results and Discussions

3.1 Drying kinetics analysis

Figure 3 indicates the variation of dimensionless moisture with time. The results show that air temperature and velocity significantly influence drying time; the temperature has a more significant effect. The average drying time is about 2.5–5.167 hours. The drying time of the mode with 70^{o}C temperature is about 1.33–1.38 and 1.72–1.87 times lower than the mode with 60^{o}C and 50^{o}C temperatures. The time drying of mode with 2 m/s air velocity decreases by 1.04–1.1 and 1.1–1.2 times compared with those in the mode with 1.5 m/s and 1 m/s air velocity at the same temperature. The highest error of dimensionless moisture was found to be 0.34%. The drying time decreases with increasing air velocity and temperature, and this trend fits with the drying theory. The correlation of drying time with air velocity and temperature is shown in Eq.14. The correlation coefficient and the maximum error of the predicted and experimental values were found to be R^2 = 0.996 and $\pm$ 3%, respectively.

t = 96577. exp(-0.15547V-0.0293746T), with R^2 = 0.996. (14)

where t (s), V (m/s), and T (^{o}C) are drying time, air velocity, and drying temperature, respectively.

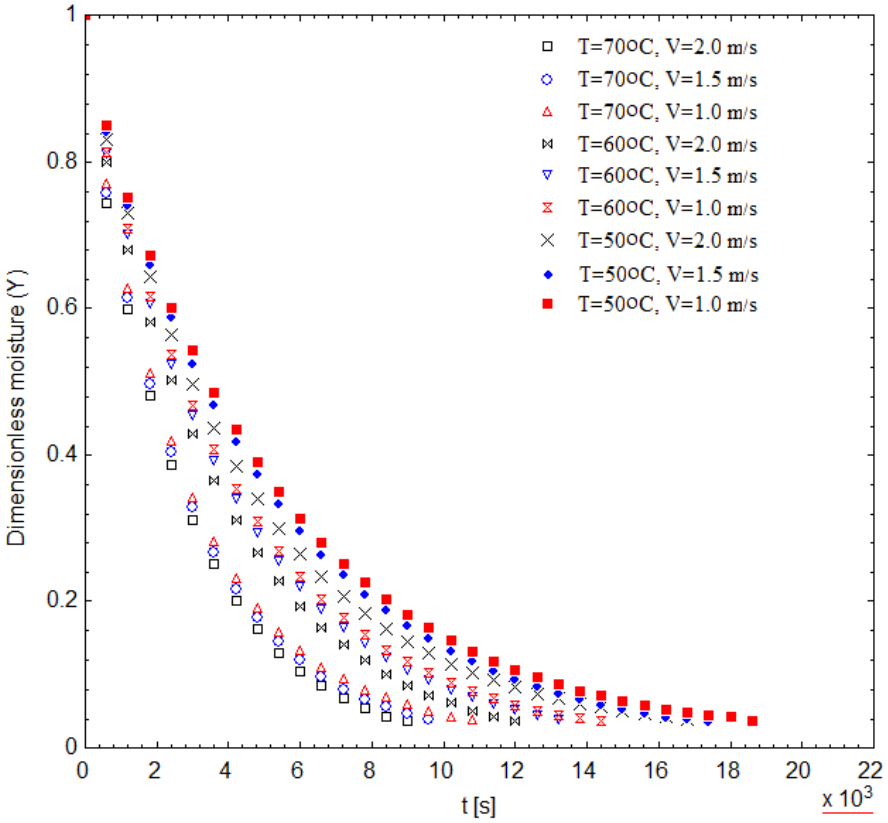

Fig. 3. The variation of dimensionless moisture with time (drying curve)

Among the five thin-layer drying models used for the survey, the Page model was the best model to describe the drying behavior of the modes, with the highest R^2 and smallest RMSE and χ^2 (see Table 1). All Page models have a correlation coefficient of $R^2 > 0.9992$, with maximum error is 5.8%. This result is consistent with the report of Zang *et al.,* [4] on modeling thin-layer drying of burdock root in a convective dryer at the mode of 1 m/s air velocity and 50–80°C drying temperature. Furthermore, few reports show that the Page model best describes the moisture reduction process for a few types of sliced tuber and sliced fruit in the drying process [24-26]. Therefore, the present work results can be trusted.

Table 1
The regression models for the drying cases

T (°C)	V (m/s)	Model	Regression parameters	R^2	RMSE	$\chi^2 x\ 10^4$
70	2.0	1	m = 0.961326; s = 0.000401348; b = 0.0162002	0.9986	0.01145	1.3996
		2	a = -0.000277614; b = 1.98789 x 10^{-8}	0.9604	0.05850	36.508
		3	s = 0.00039324	0.9907	0.01564	2.6106
		4	m = 0.970297; s = 0.000381211	0.9981	0.01266	1.7103
		5	**s = 0.000833392; n = 0.906794**	**0.9996**	**0.00614**	**0.4018**
	1.5	1	m = 0.956986; s = 0.000383521; b = 0.0220189	0.9989	0.00999	1.0614
		2	a = -0.000261487; b = 1.76756 x 10^{-8}	0.9591	0.05859	36.471
		3	s = 0.000369215	0.9967	0.01604	2.7328
		4	m = 0.968748; s = 0.000357248	0.9997	0.01285	1.7557
		5	**s = 0.000804966; n = 0.904029**	**0.9998**	**0.00412**	**0.1803**
	1.0	1	m = 0.953508; s = 0.000373647; b = 0.0278882	0.9992	0.00807	0.6877
		2	a = -0.000242171; b = 1.49606 x 10^{-8}	0.9487	0.06418	43.478
		3	s = 0.000352162	0.9961	0.01714	3.1001
		4	m = 0.966857; s = 0.000339996	0.9975	0.01413	2.1083
		5	**s = 0.000816779; n = 0.89695**	**0.9998**	**0.00333**	**0.1173**
60	2.0	1	m = 0.963804; s = 0.000278987; b = 0.00766007	0.9987	0.01047	1.1509
		2	a = -0.000203169; b = 1.07571 x 10^{-8}	0.9648	0.05293	29.418
		3	s = 0.00028178	0.9972	0.01445	2.1925
		4	m = 0.967916; s = 0.000272429	0.9986	0.01052	1.1617
		5	**s = 0.000572991; n = 0.915341**	**0.9992**	**0.00788**	**0.6513**
	1.5	1	m = 0.958847; s = 0.000259424; b = 0.0125852	0.9989	0.00955	0.9538
		2	a = -0.000186385; b = 0.905383 x 10^{-8}	0.9629	0.05349	29.912
		3	s = 0.000258634	0.9970	0.01476	2.2778
		4	m = 0.965322; s = 0.000249313	0.9986	0.01051	1.1558
		5	**s = 0.00054749; n = 0.91141**	**0.9994**	**0.00652**	**0.4445**
	1.0	1	m = 0.957107; s = 0.000247568; b = 0.0118531	0.9988	0.00967	0.9742
		2	a = -0.00017514; b = 0.791308 x 10^{-8}	0.9575	0.05657	33.334
		3	s = 0.000247779	0.9968	0.01519	2.4029
		4	m = 0.962855; s = 0.00023824	0.9986	0.01039	1.2376
		5	**s = 0.000542778; n = 0.907941**	**0.9994**	**0.00681**	**0.4834**
50	2.0	1	m = 0.949689; s = 0.000230831; b = 0.0229123	0.9992	0.00756	0.5927
		2	a = -0.000155037; b = 0.615871 x 10^{-8}	0.9489	0.06054	37.963
		3	s = 0.000210818	0.9947	0.01912	3.7859
		4	m = 0.959388; s = 0.0002135	0.9981	0.01163	1.4004
		5	**s = 0.000525381; n = 0.900587**	**0.9998**	**0.00414**	**0.1778**
	1.5	1	m = 0.954124; s = 0.000203998; b = 0.0121095	0.9989	0.00903	0.8432
		2	a = -0.000145022; b = 0.543445 x 10^{-8}	0.9561	0.05627	32.754
		3	s = 0.000204669	0.9966	0.01539	2.4497
		4	m = 0.959734; s = 0.00019610	0.9986	0.00985	1.0033
		5	**s = 0.000460902; n = 0.906809**	**0.9994**	**0.00617**	**0.3941**
	1.0	1	m = 0.952803; s = 0.000196245; b = 0.0153447	0.9991	0.00821	0.6959
		2	a = -0.000137249; b = 0.485453 x 10^{-8}	0.9543	0.05698	33.516
		3	s = 0.000194714	0.9966	0.01528	2.4093
		4	m = 0.959587; s = 0.00018651	0.9986	0.00982	0.9947
		5	**s = 0.000445929; n = 0.905377**	**0.9996**	**0.00513**	**0.2721**

*1–Logarithmic model; 2–Wang and Singh model; 3–Lewis model; 4–Henderson and Pabis model; 5–Page model

Figure 4 indicates that the drying coefficient parameters and flag coefficient are determined through experimental data. These coefficients are used to determine the mass transfer coefficients in the Bi-Di correlation. The data of the regression curves shows that the highest drying coefficient occurs at high air temperature and velocity; this parameter characterizes the drying capacity of solids

in a unit of time. Therefore, the drying process is faster at high air temperatures and velocity. The mass transfer coefficients for experimental cases are shown in Table 2. The mass transfer coefficient is determined by Bi-Di correlation with $0.1 \leq Bi \leq 100$. There are three cases with $Bi < 0.1$; the difference is insignificant, so the Bi-Di correlation is still used in these cases. The results show that the moisture diffusivity and moisture transfer coefficient are 3.452×10^{-9}–1.8516×10^{-8} m^2/s and 1.3256×10^{-7}–7.8375×10^{-7} m/s, respectively. The maximum errors in moisture diffusivity and moisture transfer coefficient were 19.97% and 23.99%, respectively. The moisture diffusivity coefficient of the mode with 70°C temperature is about 1.79–2.04 and 3.38–4.76 times better than the mode with 60°C and 50°C temperature at the same air velocity. The moisture transfer coefficient of the mode with 70°C temperature increases by 2.03–2.33 and 4.23–5.91 times compared with the mode with 60°C and 50°C temperatures. The mass transfer coefficient increases with increasing drying temperature and air velocity. This result may be that when burdock root slices are dried at high temperature, the drying sample receives more heat energy leading to increased movement of water molecules and moisture diffusivity. Furthermore, when drying burdock root at high-air velocity, moisture can be quickly removed from the surface of the drying sample, which maintains the high-pressure gradient between the surface and the air, thereby promoting the diffusion process inside the material.

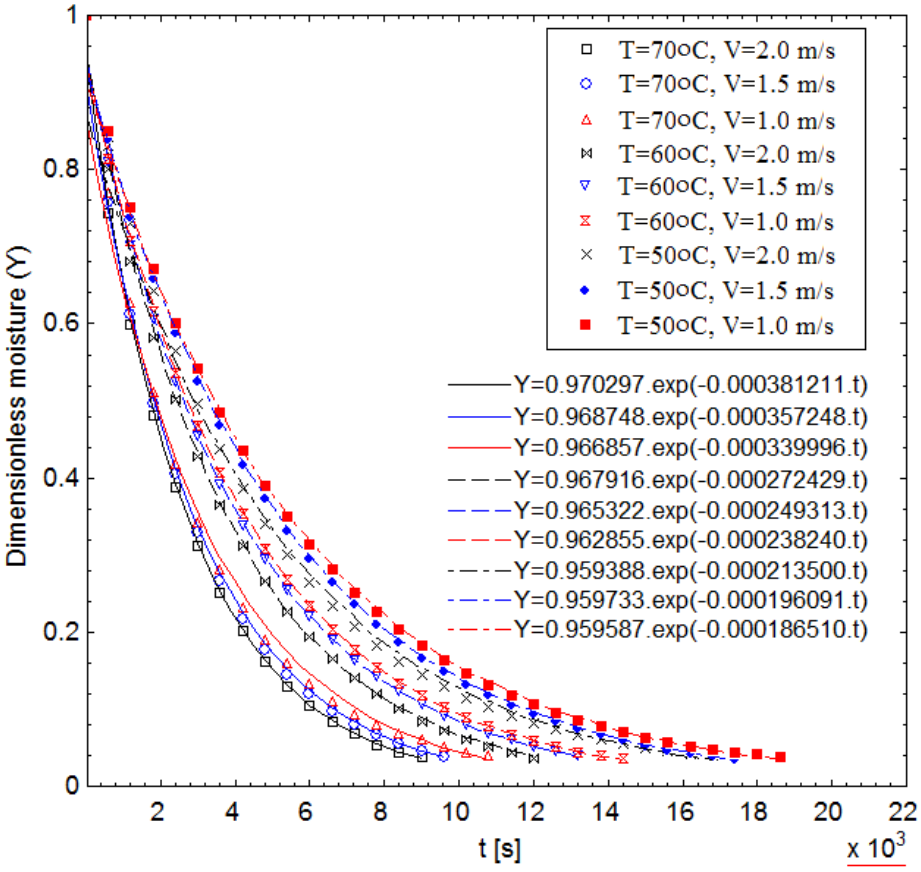

Fig. 4. The drying coefficient (s) and lag coefficient (C) in the Bi-Di correlation

Table 2
The mass transfer coefficient of burdock root

T(°C)	*V (m/s)*	*C*	*s*	*Di*	*Bi*	*D_e (m^2/s)*	*h_m (m/s)*
70	2.0	0.970297	0.000381211	2.099×10^6	0.1058	1.8516×10^{-8}	7.8375×10^{-7}
	1.5	0.968748	0.000357248	1.680×10^6	0.1150	1.4749×10^{-8}	6.7871×10^{-7}
	1.0	0.966857	0.000339996	1.176×10^6	0.1315	1.1657×10^{-8}	6.1302×10^{-7}
60	2.0	0.967916	0.000272429	2.937×10^6	0.0933	1.0348×10^{-8}	3.8617×10^{-7}
	1.5	0.965322	0.000249300	2.407×10^6	0.1005	7.4163×10^{-9}	2.9820×10^{-7}
	1.0	0.962855	0.000238200	1.679×10^6	0.1150	5.7214×10^{-9}	2.6329×10^{-7}
50	2.0	0.959388	0.000213500	3.747×10^6	0.0851	3.8922×10^{-9}	1.3256×10^{-7}
	1.5	0.959734	0.000196100	3.060×10^6	0.0919	3.6705×10^{-9}	1.3488×10^{-7}
	1.0	0.959587	0.000186510	2.145×10^6	0.1050	3.4520×10^{-9}	1.4493×10^{-7}

Figure 5 demonstrates the validation of dimensionless moisture determined by the Bi-Di correlation with experimental data. The results show that the correlation coefficient between the model and the experiment value is $R^2 > 0.9991$. The maximum average error was 8.5% for the drying cases. It shows a good agreement between the Bi-Di model and the experimental data. Therefore, the calculated results of the mass transfer coefficient according to the Bi-Di correlation can be trusted in this study.

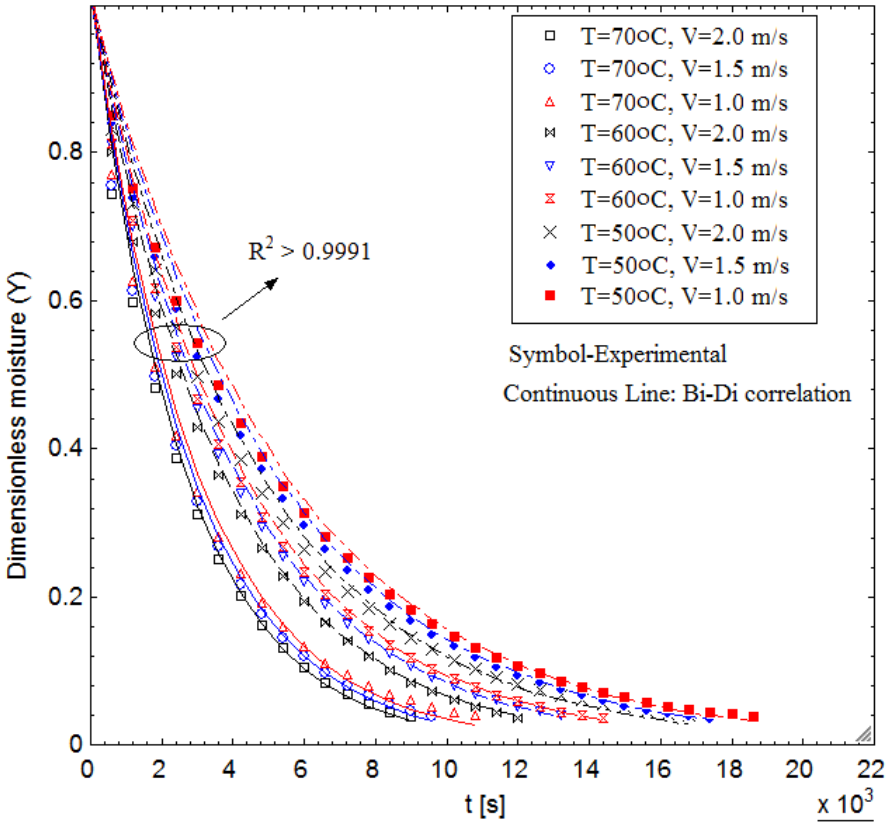

Fig. 5. The validation for the Bi-Di correlation and the experimental data

Table 3 shows the moisture diffusivity coefficient of burdock root slices and some materials under different drying conditions. The results show that the moisture diffusivity coefficient of the burdock root slices is lower than the moisture diffusivity coefficient of beetroot slices and broccoli, but larger than the moisture diffusivity coefficient of banana slices, persimmon slices, pear slices, and mango

ginger. It is due to the influence of drying conditions, material thickness, and material physicochemical properties.

Table 3
The moisture diffusivity coefficient of burdock root slices and some materials under different drying conditions

Material	Drying temperature (°C)	Air velocity (m/s)	Sample thickness (mm)	Moisture diffusivity coefficient (m^2/s)	Reference
Burdock root slices	50–70	1–2	4	3.452×10^{-9}–1.8516×10^{-8}	Present work
Banana slices	70–100	1.3	3	8.500×10^{-11}–2.290×10^{-10}	[27]
Broccoli	50–75	1.2–2.25	–	3.578×10^{-6}–16.667×10^{-6}	[11]
Persimmon slices	50–70	2	3–8	7.05×10^{-11}–2.34×10^{-10}	[28]
Mango ginger	40–70	0.84–2.25	1.77	3.70×10^{-10}–1.25×10^{-9}	[29]
Pear slices	50–71	2	5	8.56×10^{-11}–2.25×10^{-10}	[30]
Beetroot slices	50–120	2	7	3.01×10^{-9}–7.21×10^{-7}	[31]

3.2 Moisture Distribution Simulation

The mass transfer coefficient is an essential parameter in describing moisture distribution inside materials. In this part, a numerical simulation is performed to consider the moisture distribution based on the mass transfer coefficient data. Per measured practice, the slice thickness is not changed, and the slice diameter shrinkage is about 1.6 times. In order to reduce the error between simulation and experiment data, a physical model with the average dimension of the initial and final times was selected. A typical computational domain with an 18 mm slice diameter and 5 mm slice thickness is used for the simulation. The physical model and input data corresponding to the drying mode of 70°C, 2 m/s are illustrated in Figure 6. The input data is used in numerical simulation: $D_e = 1.8516 \times 10^{-8}$ m^2/s; $h_m = 7.8375 \times 10^{-7}$ m/s; $M_i = 3.4053$. Assume that the material is the homogeneous, isotropic, and uniform distribution of initial moisture in the material.

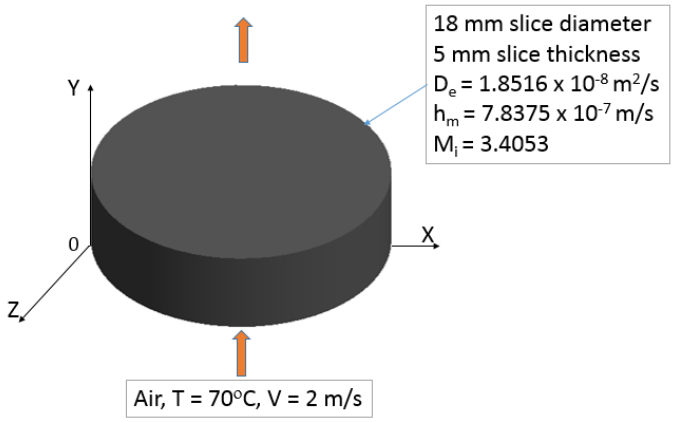

Fig. 6. The physical model and input data

The equations are used in numerical simulation

The Fick's second law for moisture diffusion [17]

$$\frac{\partial M}{\partial t} = D_e \nabla^2 M \tag{15}$$

The boundary condition

At the initial time: t = 0→ M_i = 3.4053 (16)

At surface [8, 9]: $D_e \nabla^2 M = h_m(M_s - M_e)$ (17)

where M_e is the equilibrium moisture content, it is usually tiny and determined experimentally. This simulation assumes that equilibrium moisture content is ignored and accepts the errors in the simulation results. M_s is moisture content at the surface.

A numerical simulation for *transient mass transfer* was performed based on the analogy between heat and mass transfer. The double precision, tetrahedral mesh, and refinement mesh at the outer wall are used to improve the accuracy of the simulation results. The tetrahedral mesh and refinement mesh generation can see in Figure 7. The 0.5–0.3 mm mesh sizes and 1–0.05 s time step are used to test the grid and time step independence. It takes more than 4 hours to simulate 5 minutes of drying with setup 0.05 s time step. Therefore, the time step only tests in the range of 1–0.05 s. The results show that the deviation of the moisture content dry basis of the setup with 1 s time step and 0.5 mm mesh size is negligible compared with those in the setup with 0.05 s time step and 0.3 mm mesh size (see Table 4). Therefore the mesh size of 0.5 mm and the time step of 1 s are chosen to reduce the simulation time.

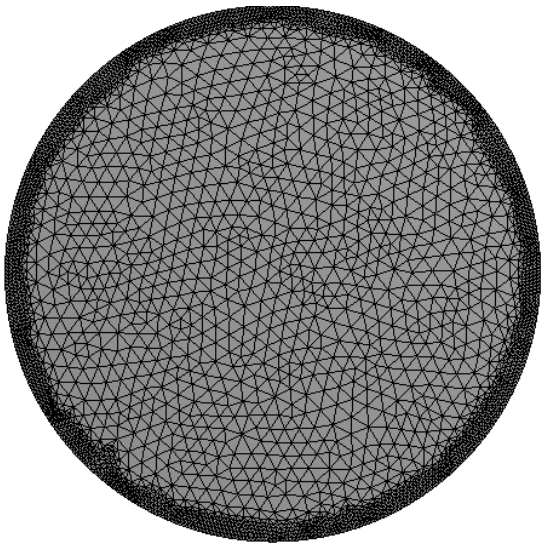

Fig. 7. Generate the tetrahedral mesh and refinement mesh at the outer wall

Table 4
The grid and time step independence test after five minutes simulation

No.	Mesh size	Elements	Time step	M	Error
1	0.5	724,135	1 s	2.95951	0.0152%
2	0.4	1,109,860	1 s	2.95949	0.0145%
3	0.3	1,983,754	1 s	2.95947	0.0139%
4	0.3	1,983,754	0.5 s	2.95930	0.0081%
5	0.3	1,983,754	0.1 s	2.95909	0.0010%
6	0.3	1,983,754	0.05 s	2.95906	–

Figure 8 shows the moisture distribution inside the slice at times from 30 to 110 minutes. The results show that the moisture content of the material decreases with the drying time; the farther the layer is from the center, the lower the moisture content. The moisture gradient is radial, opposite to the direction of moisture flow, which is entirely consistent with the theory of drying. The moisture distribution symmetrically through the plane XZ at Y = 2.5 mm. It is due to the assumption of uniformity, isotropy, and uniform in the initial moisture distribution of material and homogeneous boundary conditions (thin-layer drying theory).

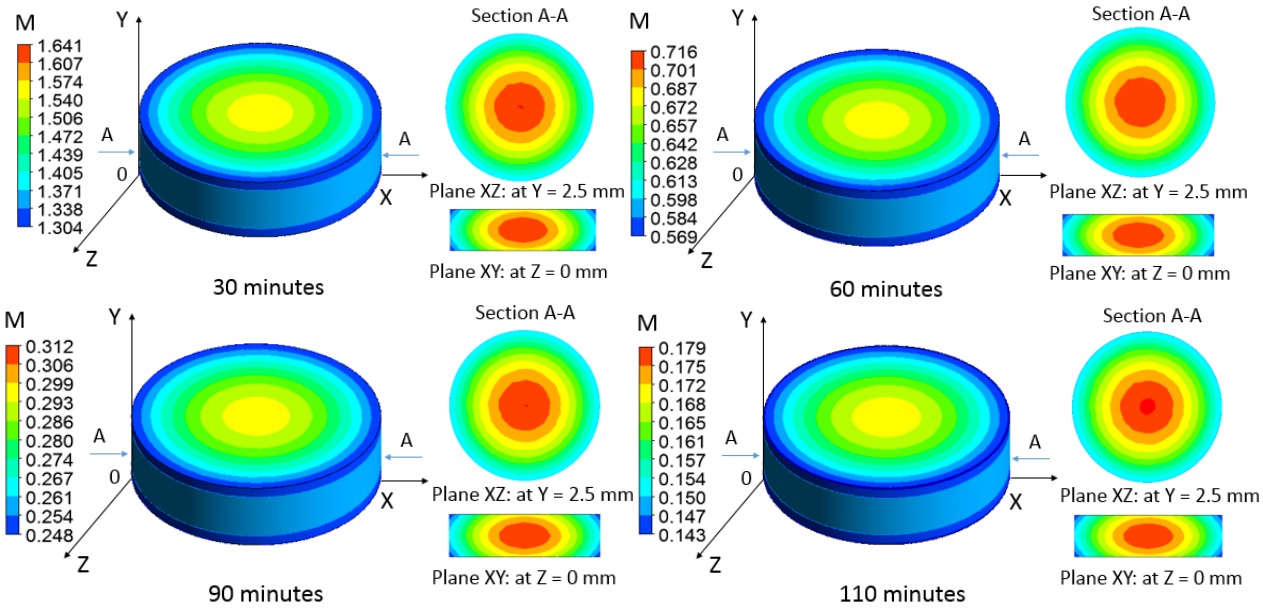

Fig. 8. The moisture distribution inside the burdock root slice at times from 30 to 110 minutes

Figure 9 shows the moisture distribution at the time of 120 minutes. The results show the highest moisture content of 0.136 at the center and the smallest of 0.108 at the outer shell. The isohumidity curves are almost concentrically distributed in layers. The regions with moisture greater than 0.108 d.b tend to expand in layers towards the center. The process of moisture drainage takes place intensely and evenly through 2 planes XZ at Y = 0 mm and Y = 5 mm (this is the direction with the small thickness).

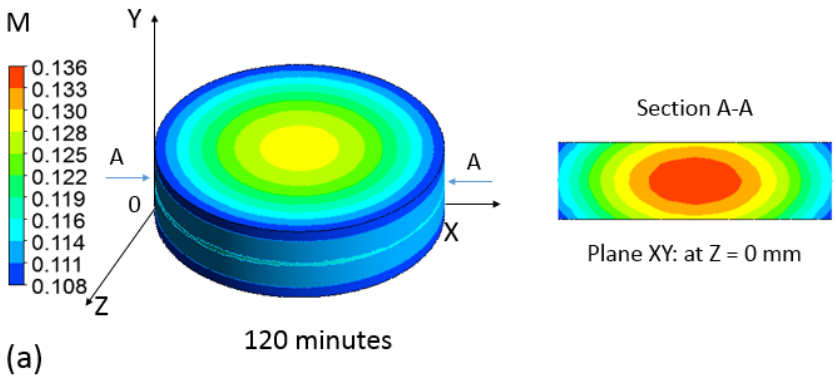

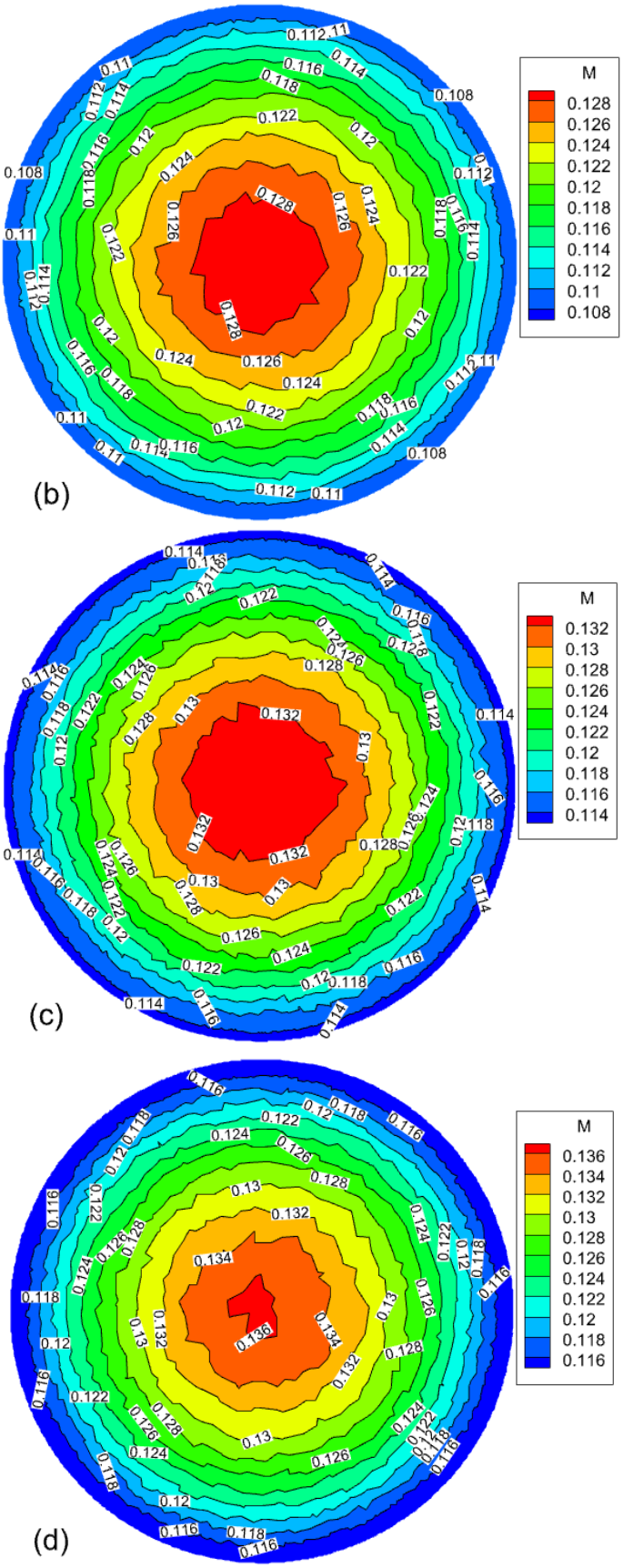

Fig. 9. Moisture distribution at the time of 120 minutes (a) shell and plane XY at Z = 0 mm (b) plane XZ at Y = 0 mm (c) plane XZ at Y = 1.25 mm (d) plane XZ at Y = 2.5 mm

Figure 10 shows the drying curve according to the simulation and experimental data. The results show that the correlation coefficient between simulation and experimental data is R^2 = 0.9979, and the maximum difference in the dimensionless moisture is 0.062. The difference in drying time between the simulation and experiment is 20%. The simulation result is consistent with experimental data. The errors are mainly due to assumptions regarding the neglect of shrinkage, the neglect of equilibrium moisture, and the error of the mass transfer coefficient.

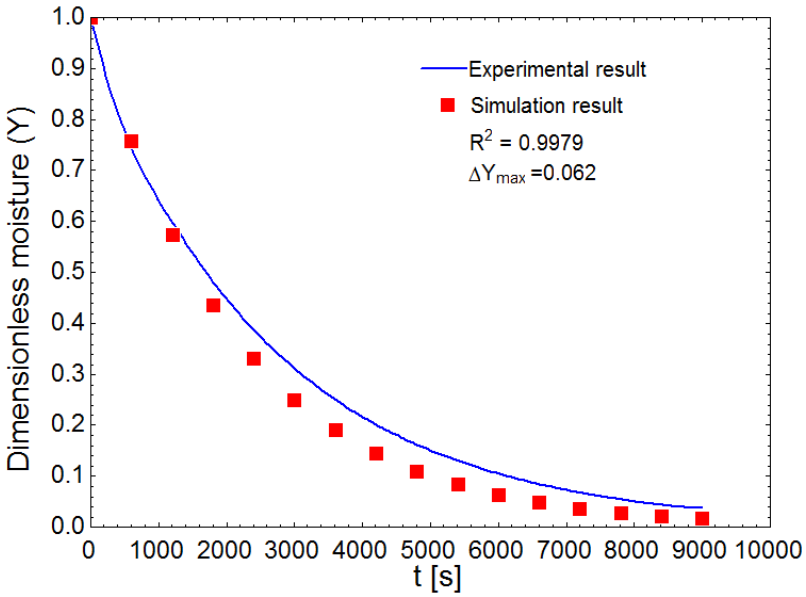

Fig. 10. The drying curve according to the simulation and experimental data

4. Conclusions

This paper investigated the thin-layer drying kinetics of Vietnam burdock root in a convective dryer with a survey scope of 50 –70°C drying temperature and 1–2 m/s air velocity. The study results show that the mass transfer coefficient increases with increasing drying temperature and air velocity. The Page model was the best model to describe the drying behavior of burdock root, with a correlation coefficient of $R^2 > 0.9992$. Moisture diffusivity coefficient D_e = 3.4520 x 10^{-9}–1.8516 x 10^{-8} m^2/s, moisture transfer coefficient h_m = 1.3256 x 10^{-7}–7.8375 x 10^{-7} m/s. The maximum errors in moisture diffusivity and moisture transfer coefficient were 19.97% and 23.99%, respectively. The current work is useful for designing and operating a convective dryer to dry burdock roots.

Acknowledgement

This work belongs to the project in 2023 funded by Ho Chi Minh City University of Technology and Education, Vietnam.

References

[1] Yuk-Shing Chan, Long-Ni Cheng, Jian-Hong Wu, Enoch Chan, Yiu-Wa Kwan, Simon Ming-Yuen Lee, George Pak-Heng Leung, Peter Hoi-Fu Yu, and Shun-Wan Chan. "A review of the pharmacological effects of Arctium lappa (burdock)." *Inflammopharmacology* 19, no. 5 (2011): 245-254. https://doi.org/10.1007/s10787-010-0062-4.

[2] Yi Lu, Min Zhang, Jincai Sun, Xinfeng Cheng, and Benu Adhikari. "Drying of burdock root cubes using a microwave-assisted pulsed spouted bed dryer and quality evaluation of the dried cubes." *Drying Technology* 32, no. 15 (2014): 1785-1790. https://doi.org/10.1080/07373937.2014.945180.

[3] Junjie Xia, Zili Guo, Sheng Fang, Jinping Gu, and Xianrui Liang. "Effect of drying methods on volatile compounds of burdock (Arctium lappa L.) root tea as revealed by gas chromatography mass spectrometry-based metabolomics." *Foods* 10, no. 4 (2021): 868. https://doi.org/10.3390/foods10040868.

[4] Bin Zhang, Meng Li, Yiteng Qiao, Peng Gao, Lingyu Li, and Zhenjia Zheng. "Potential use of low-field nuclear magnetic resonance to determine the drying characteristics and quality of Arctium lappa L. in hot-blast air." *Lwt* 132 (2020): 109829. https://doi.org/10.1016/j.lwt.2020.109829.

[5] Ehsan Kianpour, Nor Azwadi Che Sidik, Seyyed Muhammad Hossein Razavi Dehkordi, and Siti Nurul Akmal Yusof. "Numerical Simulation of Steady and Unsteady Flow and Entropy Generation by Nanofluid Within a Sinusoidal Channel." *Journal of Advanced Research in Fluid Mechanics and Thermal Sciences* 89, no. 2 (2022): 25-42. https://doi.org/10.37934/arfmts.89.2.2542.

[6] Nguyen Thanh LuanNguyen Minh Phu. "Thermohydraulic Performance and Entropy Generation of Baffled Channel: Numerical Analysis and Optimization." *Journal of Thermophysics and Heat Transfer* 36, no. 2 (2022): 303-313. https://doi.org/10.2514/1.T6332.

[7] Aly, Hossam S., Yehia A. Eldrainy, Tholudin M. Lazim, and Mohammad Nazri Mohd Jaafar. "On the contribution of drag and turbulent stresses in the fragmentation of liquid droplets: a computational study." *CFD Letters* 2, no. 2 (2010): 97-105.

[8] Minh Phu Nguyen, Tu Thien Ngo, and Thanh Danh Le. "Experimental and numerical investigation of transport phenomena and kinetics for convective shrimp drying." *Case Studies in Thermal Engineering* 14 (2019): 100465. https://doi.org/10.1016/j.csite.2019.100465.

[9] Chalida Niamnuy, Sakamon Devahastin, Somchart Soponronnarit, and GS Vijaya Raghavan. "Modeling coupled transport phenomena and mechanical deformation of shrimp during drying in a jet spouted bed dryer." *Chemical Engineering Science* 63, no. 22 (2008): 5503-5512. https://doi.org/10.1016/j.ces.2008.07.031.

[10] I DincerMM Hussain. "Development of a new Bi–Di correlation for solids drying." *International Journal of Heat and Mass Transfer* 45, no. 15 (2002): 3065-3069. https://doi.org/10.1016/S0017-9310(02)00031-5.

[11] Vlatka Mrkić, Marko Ukrainczyk, and Branko Tripalo. "Applicability of moisture transfer Bi–Di correlation for convective drying of broccoli." *Journal of Food Engineering* 79, no. 2 (2007): 640-646. https://doi.org/10.1016/j.jfoodeng.2006.01.078.

[12] Hao-Yu Ju, Hamed M El-Mashad, Xiao-Ming Fang, Zhongli Pan, Hong-Wei Xiao, Yan-Hong Liu, and Zhen-Jiang Gao. "Drying characteristics and modeling of yam slices under different relative humidity conditions." *Drying Technology* 34, no. 3 (2016): 296-306. https://doi.org/10.1080/07373937.2015.1052082.

[13] Izaora Mwamba, Karl Tshimenga, J Kayolo, L Mulumba, G Gitago, CM Tshibad, J Noël, and M Kanyinda. "Comparison of two drying methods of mango (oven and solar drying)." *MOJ Food Process Technol* 5, no. 1 (2017): 240-243. https://doi.org/10.15406/mojfpt.2017.05.00118.

[14] Francisco J Gómez-de la Cruz, José M Palomar-Carnicero, Quetzalcoatl Hernández-Escobedo, and Fernando Cruz-Peragón. "Determination of the drying rate and effective diffusivity coefficients during convective drying of two-phase olive mill waste at rotary dryers drying conditions for their application." *Renewable Energy* 153 (2020): 900-910. https://doi.org/10.1016/j.renene.2020.02.062.

[15] Paddy Likhayo, Anani Y Bruce, Tadele Tefera, and Jones Mueke. "Maize grain stored in hermetic bags: Effect of moisture and pest infestation on grain quality." *Journal of Food Quality* 2018 (2018): 1-9. https://doi.org/10.1155/2018/2515698.

[16] Nguyen Thanh Luan, Nguyen Minh Ha, and Lai Hoai Nam. "Research the efficiency of gravity heat pipe with R134a refrigerant on cabinet dryer." *Journal of Technical Education Science*, no. 64 (2021): 88-98. https://doi.org/10.54644/jte.64.2021.98.

[17] Dimitrios A Tzempelikos, Alexandros P Vouros, Achilleas V Bardakas, Andronikos E Filios, and Dionissios P Margaris. "Case studies on the effect of the air drying conditions on the convective drying of quinces." *Case Studies in Thermal Engineering* 3 (2014): 79-85. https://doi.org/10.1016/j.csite.2014.05.001.

[18] Doan Thi Hong Hai, Nguyen Van Dung, and Nguyen Minh Phu. "Experimental Determination of Transport Parameters of Dragon Fruit Slices by Infrared Drying." *Journal of Advanced Research in Fluid Mechanics and Thermal Sciences* 97, no. 2 (2022): 80-90.

[19] Daniel I Onwude, Norhashila Hashim, Rimfiel B Janius, Nazmi Mat Nawi, and Khalina Abdan. "Modeling the thin-layer drying of fruits and vegetables: A review." *Comprehensive reviews in food science and food safety* 15, no. 3 (2016): 599-618. https://doi.org/10.1111/1541-4337.12196.

[20] XV Statgraphics Centurion. "version 15.2. 14; software for technical computation; StatPoint Technologies." *Inc.: Warrenton, VA, USA* (2010).

[21] Tuncay Gunhan, Vedat Demir, Ebru Hancioglu, and Arif Hepbasli. "Mathematical modelling of drying of bay leaves." *Energy Conversion and Management* 46, no. 11-12 (2005): 1667-1679. https://doi.org/10.1016/j.enconman.2004.10.001.

[22] Barry N TaylorChris E Kuyatt, *Guidelines for evaluating and expressing the uncertainty of NIST measurement results*. Vol. 1297. 1994: US Department of Commerce, Technology Administration.
[23] Sanford A KleinF Alvarado. "Engineering equation solver software (EES)." *F-Chart Software: Madison, WI, USA* (2013).
[24] Adekanmi Olusegun Abioye, Adefemiwa Ayobami Adekunle, Olorunfemi Adebisi Jeremiah, Ibrahim Olajide Bazambo, Oluwakemi Busayo Adetoro, Khafayat Oluwadamilola Mustapha, Chioma Favour Onyeka, and Thomas Adedayo Ayorinde. "Modelling the influence of hot air on the drying kinetics of turmeric slices." *Croatian journal of food science and technology* 13, no. 2 (2021): 167-175. https://doi.org/10.17508/CJFST.2021.13.2.05.
[25] Raquel PF Guiné, Susana Pinho, and Maria João Barroca. "Study of the convective drying of pumpkin (Cucurbita maxima)." *Food and bioproducts processing* 89, no. 4 (2011): 422-428. https://doi.org/10.1016/j.fbp.2010.09.001.
[26] CL HiiJEREMIAH F Ogugo. "Effect of pre-treatment on the drying kinetics and product quality of star fruit slices." *Journal of Engineering Science and Technology* 9, no. 1 (2014): 123-135.
[27] Ratiya Thuwapanichayanan, Somkiat Prachayawarakorn, Jaruwan Kunwisawa, and Somchart Soponronnarit. "Determination of effective moisture diffusivity and assessment of quality attributes of banana slices during drying." *LWT-Food Science and Technology* 44, no. 6 (2011): 1502-1510. https://doi.org/10.1016/j.lwt.2011.01.003.
[28] İbrahim Doymaz. "Evaluation of some thin-layer drying models of persimmon slices (Diospyros kaki L.)." *Energy conversion and management* 56 (2012): 199-205. https://doi.org/10.1016/j.enconman.2011.11.027.
[29] Thirupathihalli Pandurangappa Krishna MurthyBalaraman Manohar. "Hot air drying characteristics of mango ginger: Prediction of drying kinetics by mathematical modeling and artificial neural network." *Journal of Food Science and Technology* 51 (2014): 3712-3721. https://doi.org/10.1007/s13197-013-0941-y.
[30] İbrahim Doymaz. "Experimental study on drying of pear slices in a convective dryer." *International Journal of Food Science & Technology* 48, no. 9 (2013): 1909-1915. https://doi.org/10.1111/ijfs.12170.
[31] SV GokhaleSS Lele. "Dehydration of red beet root (Beta vulgaris) by hot air drying: Process optimization and mathematical modeling." *Food Science and Biotechnology* 20, no. 4 (2011): 955. https://doi.org/10.1007/s10068-011-0132-4